

Optical Frequency Trapped Ion Probe for a Varying Proton-to-Electron Mass Ratio

Mark G. Kokish,¹ Patrick R. Stollenwerk,¹ Masatoshi Kajita,² and Brian C. Odom^{1,*}

¹*Department of Physics and Astronomy, Northwestern University, Evanston, Illinois 60208, USA*

²*National Institute of Information and Communications Technology, Koganei, Tokyo 184-8795, Japan*

(Dated: October 25, 2017)

Molecules with deep potential wells provide optical transitions sensitive to variation in the proton-to-electron mass ratio (μ). Here we propose the molecular ion TeH^+ as a favorable candidate for an improved laboratory search for changing μ . We identify narrow-linewidth vibrational overtones in TeH^+ with high absolute sensitivity to μ . TeH^+ additionally provides electronic transitions with highly diagonal Franck-Condon factors. This allows for the implementation of optical state preparation schemes faster than the spectroscopy state lifetimes, allowing a single-ion spectroscopy experiment to reach the projection-noise limited statistical uncertainty of 5×10^{-18} with one day of averaging. In addition, we analyze the extent of Stark and Zeeman systematic shifts. We show that the spectroscopy states within the ground X_10^+ electronic manifold are relatively insensitive to external fields, leading to a fractional precision $< 1 \times 10^{-18}$ using reasonable methods of external field control previously demonstrated in ion trap experiments.

Searches for variation of fundamental constants are well motivated by their ability to probe mechanisms beyond the Standard Model [1]. Modern laboratory searches take advantage of precise measurements of atomic frequencies that access the fine structure constant (α) and the proton-to-electron mass ratio (μ) [2]. Setting new constraints on the variation of μ is especially intriguing as it is predicted to drift faster than α [3]. The tightest constraint on the variation of μ , measured by astronomical observations of methanol, is $2.4 \times 10^{-17}/\text{yr}$ [4]. In contrast, the tightest laboratory constraint on the fractional variation of μ , $\sim 1 \times 10^{-16}/\text{yr}$, was obtained from a comparison of hyperfine and electronic transitions in atomic clocks [5, 6]. However, since the sensitivity to μ arises from the relatively low frequency microwave hyperfine transition, it will be challenging to significantly improve the precision of μ variation searches by this approach. In order to surpass the limits set by microwave clocks, many have proposed to take advantage of the internal structure of molecules.

Compared to hyperfine transitions in atoms, highly excited vibration levels have similar relative sensitivity to μ , but with frequencies of 10-1000 THz, resulting in orders of magnitude larger absolute sensitivity [7, 8]. One technique for using these states in a measurement is to drive a transition to a nearby level with different μ sensitivity [7–11]. Since the spectroscopy frequency is reduced without loss of sensitivity to μ , this approach enables high-sensitivity probes using low-frequency spectroscopy and also reduces Doppler shift uncertainties [7, 8]. However, because the states involved will generally have quite different character, this approach can create challenges in controlling differential systematic shifts to the desired level.

An alternative approach is to directly measure vibrational overtone frequencies in molecules, with previous

proposals suggesting performing the spectroscopy using stimulated Raman transitions [12, 13]. Here we propose taking advantage of the deep potential well in the tellurium monohydride cation (TeH^+) to drive a single-photon optical transition with high sensitivity to μ . In comparison to Raman transitions in the optical domain, single photon transitions do not require a frequency comb for stabilization, and light shifts pose a significantly reduced challenge. Our proposed spectroscopy states are each relatively insensitive to many systematic frequency shifts, and certain important differential shifts are further reduced because of the similar electronic and rovibrational character of the two states.

Measurement of overtones in trapped ions is currently an active area of research [14, 15]. Additionally, recent demonstrations of molecular ion quantum state preparation [16–20] and non-destructive state readout [19, 21] suggest that spectroscopy on a single trapped molecular ion might be able to fully take advantage of the favorable systematic uncertainties we predict for TeH^+ . Additionally, we find that the state lifetimes are sufficiently long that statistical uncertainties of single-ion spectroscopy can also be acceptably low, potentially allowing for probing variation of μ at a level better than $10^{-17}/\text{yr}$.

A number of favorable properties of TeH^+ stem from its unique electronic structure, which has recently been calculated [22] but has not yet been experimentally measured. In the absence of spin-orbit coupling ($\Lambda + S$ picture), the ground state is $^3\Sigma^-$, and the two lowest excited states correspond to $^1\Delta$ and $^1\Sigma^+$ states. However, strong spin-orbit coupling originating from the heavy tellurium atom makes Hund’s case (c) the most natural basis [23] (Fig. 1).

Spin-orbit coupling in TeH^+ leads to two significant properties for the low lying electronic states. First, the ground $^3\Sigma^-$ state is split by a large 1049 cm^{-1} interval, producing two independent electronic states with different Ω . The X_10^+ state is insensitive to certain systematic frequency shifts. Second, spin-orbit coupling relaxes the selection rules that would prevent transitions between the

* b-odom@northwestern.edu

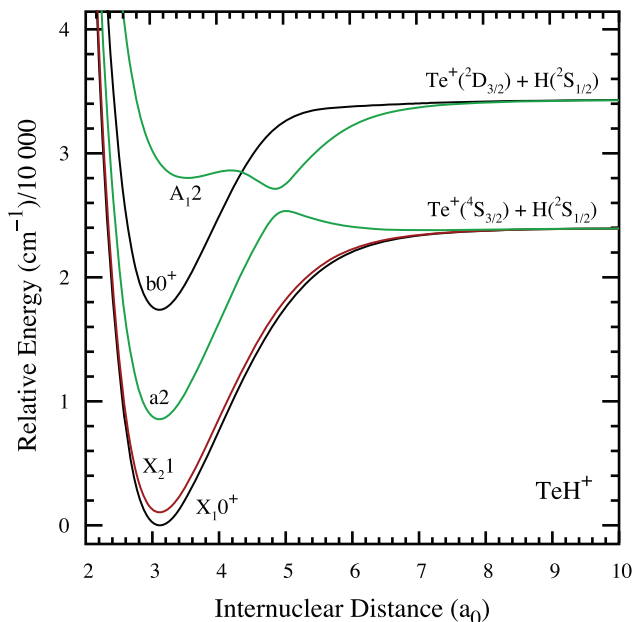


FIG. 1: Low lying electronic states of TeH^+ . Figure adapted from [22].

three low lying states in the $\Lambda + S$ picture. This yields relatively short excited state lifetimes of $15 \mu\text{s}$ and 2.4 ms for the b_0^+ and a_2 states, respectively, calculated using LEVEL 16 [24].

The X_1^0+ , X_2^1 , a_2 , and b_0^+ electronic states correspond to different orbital and spin configurations of two electrons in non-bonding p orbitals localized on the tellurium ion. As a result, transitions between these states leave the equilibrium bond length and bond strength relatively unperturbed, leading to highly diagonal Franck-Condon factors (FCFs). TeH^+ additionally has a small reduced mass, leading to large predicted rotational and vibrational constants of approximately 6.2 and 2100 cm^{-1} , respectively. These relatively large spacings reduce the number of occupied states for a given temperature, only requiring tens of scattering events on average to cool TeH^+ from an excited rovibrational state. We further choose to focus on the $^{130}\text{TeH}^+$ ion, as ^{130}Te does not possess nuclear spin. The short excited state lifetimes, small phase-space volume and diagonal FCFs enable the implementation of a fast optical cooling scheme [18].

Franck-Condon factors depend most heavily on the difference in equilibrium bond length between electronic states. Having no measured constants for TeH^+ , we evaluate the accuracy of the calculations in [22] by comparing theoretical and experimental investigations of an isoelectronic species with similar mass: antimony hydride (SbH). Alekseyev et al., using a similar computation method [25], predict a difference in equilibrium bond lengths between the b and X states within a factor of two of the measured value [26]. For optical cooling, we also rely on short lifetimes. The lifetime of the b state predicted in [25] was also accurate to within a factor of

two [27]. Other properties that have a smaller impact on cooling efficiency such as harmonic frequencies, spin-orbit splittings and electronic energies were predicted within 10% [26]. Inaccuracy at this level will not significantly alter any of the favorable properties of TeH^+ that we consider here. Compared to the SbH calculation, the TeH^+ calculation explicitly treats more electrons and uses a significantly larger basis set. The TeH^+ calculation is therefore expected to be more accurate than the SbH calculation.

The absolute sensitivity of a particular overtone transition to μ depends on the shape of the electronic potential, at first increasing with vibrational energy and eventually decreasing near the dissociation limit [2, 8]. We focus here on the the properties of the ground X_1^0+ state, using the coefficients from [22]. In addition to the absolute sensitivity, we consider the statistical precision to which an overtone can be measured. For a projection noise-limited Ramsey experiment, the RMS frequency error for a single ion is given by:

$$\delta f_{rms}(T) = \frac{1}{2T_R\pi} \sqrt{\frac{T_c}{2T}} \quad (1)$$

where T_R is the Ramsey time, T_c is the cycle time and T is the total measurement time [28]. The uncertainty can be more accurately modeled by solving for the slope of the discriminant signal in a multilevel system [29–31]. Setting aside such optimization here, we set the Ramsey time to the inverse natural linewidth of the transition, Γ^{-1} . For a fixed total measurement time, we consider two limiting cases. In the limit of long cycle times, δf_{rms} is proportional to Γ , while in the limit of zero dead time ($T_c = T_R$), δf_{rms} is proportional to $\sqrt{\Gamma}$. The fractional precision of μ will then be proportional to the figure of merit [8]:

$$\frac{df}{d\mu} \frac{1}{\Gamma^k} \quad (2)$$

where $df/d\mu$ is the absolute sensitivity and k is 1 or $1/2$ for the cycle time or linewidth-limited cases, respectively. In Fig. 2 we plot the figure of merit for both cases as a function of excited vibrational state. In both cases probing higher vibrational states are advantageous, especially for experiments with high duty cycles.

In a single-ion experiment, the cycle time will be limited by the state preparation time associated with cooling each individual degree of freedom in TeH^+ . However, due to the short $15 \mu\text{s}$ lifetime of the excited b_0^+ state and the diagonal FCFs between electronic states, rapid cooling can be achieved on timescales shorter than the interrogation time using a reasonable number of commercially available lasers [32]. Given a successful implementation of a fast optical state preparation scheme, the linewidth-limited scenario suggests that driving an overtone from $v = 0$ to $v = 8$ ($f_{08} = 430 \text{ THz}$) will be the

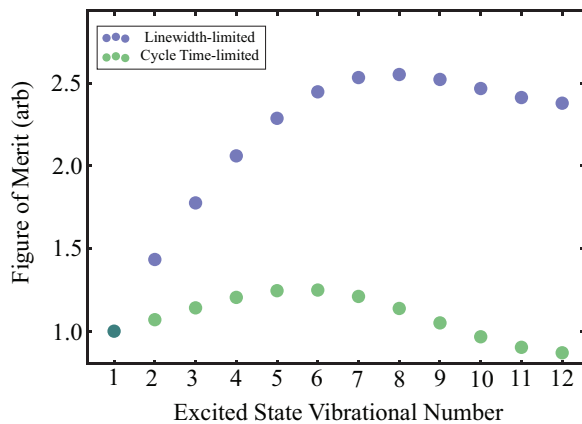


FIG. 2: Figure of merit as a function of vibrational excited state for cycle time-limited ($k = 0$) and linewidth-limited ($k = 1/2$) experiments, normalized to $v = 1$. For TeH^+ , transitions to $v = 6$ and $v = 8$ are the most optimal.

most optimal transition for probing a fractional variation in μ . In addition, a single photon transition must couple two states of opposite parity. We therefore aim to perform spectroscopy between $|X_1 0^+, v = 0, J = 0\rangle$ and $|X_1 0^+, v = 8, J = 1\rangle$. In an experiment limited by the excited state lifetime, this transition reaches a fractional statistical uncertainty of $1.3 \times 10^{-15} / \sqrt{T/s}$, or 4.5×10^{-18} with one day of averaging, corresponding to a precision of 2 mHz. The uncertainty can potentially be pushed lower by driving a similar energy overtone in TeD^+ , as the lifetime is expected to be approximately twice as long.

In order to evaluate systematic frequency shifts, we require a complete picture of the rotational and vibrational energy levels in each electronic state and the dipole moments coupling each level to each other. We input the potential energy curves and dipole moment functions computed by Gonçalves dos Santos et al. into a modified version of LEVEL 16 to generate an interaction matrix [22]. Here we analyze electric and magnetic field shifts, summarized in Tables I, II, and III.

Blackbody radiation (BBR) causes differential Stark shifts of the spectroscopy states by coupling each of them to (1) adjacent rotational states in the same vibrational manifold (2) other vibrational manifolds and (3) other electronic manifolds. BBR shifts from coupling between adjacent rotational levels and distant electronic levels can be well-approximated by an expression for Stark shifts in the high and low-frequency limits, respectively. Since vibrational frequencies and the spin-orbit splitting frequency occur in spectral regions where BBR is the strongest, neither approximation holds. In order to calculate all BBR shifts reported here, rather than using any limiting-case approximations, we use in all cases Eq. 8 of Farley and Wing [33], and calculate the BBR Stark shift numerically integrated over the entire BBR spectrum.

For unpolarized radiation, when the radiation frequency is much larger than the rotational spacing, there

TABLE I: Blackbody Radiation Shifts^a

Effect	Ground	Excited	Diff.	Diff./ f_{08}
BBR (rotation)	11.6	11.4	-0.2	-0.47
BBR (vibration)	-0.22	0.45	0.67	1.6
BBR ($b0^+$)	-0.64	-0.2	0.39	0.91
BBR (X_21)	-0.21	-0.049	0.16	0.37
Total			1.0	2.4

^a BBR at 300 K. All values in mHz except last column, the fractional shift divided by 10^{-18} .

is a fortuitous cancellation for $\Omega = 0$ levels, which renders identical the AC Stark shifts from each $|J\rangle$ within a manifold due to coupling to adjacent rotational states. This cancellation occurs because of an apparently accidental interplay between level spacing and dipole transition moments. The frequency shift of each $|J\rangle$ level is given by

$$\Delta f = \frac{2BE^2\mu_0^2}{3f_D^2h^2} \quad (3)$$

where f_D is the drive frequency, B is the rotational constant, E is the electric field amplitude and μ_0 is the dipole moment. For the lowest several rotational intervals, the effects of BBR are well approximated by this result for the high frequency limit. Because of centrifugal distortion, the shifts are slightly different in the two spectroscopy states, but the cancellation is still quite good. Using the available parameters beyond their actual accuracy, we find the differential shift between $|X_1 0^+, v = 0, J = 0\rangle$ and $|X_1 0^+, v = 8, J = 1\rangle$ at room temperature to be below 1 mHz.

For the vibrational interaction, BBR couples the $|X_1 0^+, v = 0\rangle$ level only with the neighboring $v = 1$ level, whereas the $|X_1 0^+, v = 8\rangle$ level has counteracting couplings to both $v = 7$ and $v = 9$. Therefore, we expect no cancellations in the differential Stark shift. Even so, the vibrational transition moments are sufficiently small (of order 0.1 Debye) that these Stark shifts are small. The differential shift is 0.67 mHz.

Room temperature BBR-induced interaction with $b0^+$ causes the $|X_1 0^+, v = 0, J = 0\rangle$ state to shift, dominantly due to the diagonal coupling to the $|b0^+, v = 0\rangle$ level. Similarly, the $|X_1 0^+, v = 8, J = 1\rangle$ state couples primarily to dipole-connected states in $|b0^+, v = 8\rangle$. The spin-forbidden nature of this transition leads to a small differential shift of 0.39 mHz. The BBR-induced coupling of the spectroscopy $X_1 0^+$ manifold to the nearby and diagonally coupled $X_2 1$ manifold is also dominated by $\Delta v = 0$ couplings, yielding a net differential shift of 0.16 mHz. Assuming the temperature is kept stable to within 10 K, uncertainty of the BBR shifts will be more than an order of magnitude lower than the remaining Stark and Zeeman shifts.

When multiple decay channels are open to the upper state, the laser intensity I_{sat} required to saturate the

spectroscopy transition is proportional to $\Gamma_{\text{tot}}^2/\mu^2$, where Γ_{tot} is the total relaxation rate of the upper state, and μ is the transition moment of the transition [12, 34]. In the familiar case of a 2-level system, I_{sat} is proportional to μ^2 , so a weaker transition requires less laser power to saturate. However, in the case of spectroscopy on a vibrational overtone transition Γ_{tot}^2 is dominated by other channels, and I_{sat} is inversely proportional to μ^2 , becoming larger with the Δv of the overtone. Thus, it is important to assess the size of the light shifts arising from the spectroscopy laser.

We consider the $\text{TeH}^+ |X_1 0^+, v=0, J=0\rangle \rightarrow |X_1 0^+, v=8, J=1\rangle$ transition. The upper state $\Gamma_{\text{tot}} = 25 \text{ s}^{-1}$. The spectroscopy channel has $\Gamma = 2.4 \times 10^{-4} \text{ s}^{-1}$. The intensity required to saturate this spectroscopy transition is dramatically elevated from the 2-level case but is still a quite manageable at $1.5 \mu\text{W}/\text{mm}^2$. At this drive intensity, the light shift from coupling either of the spectroscopy states to the $b0^+$ manifold is below 10 nHz, and the light shift from coupling to the $X_2 1$ manifold is two orders of magnitude below this. We conclude that even though the spectroscopy transition is far weaker than other upper state decay channels, light shifts arising from spectroscopy on this transition are too small to be of concern.

For $\Omega = 0$ states, opposing Stark coupling to the two adjacent states arising from unpolarized low-frequency fields results in a vanishing Stark shift for all but the lowest rotational level. However, DC Stark shifts, e.g., arising from uncompensated patch potentials on the electrodes, are polarized, so this cancellation is not immediately useful. Note, though, that at the cost of experimental overhead, it would be possible to effectively unpolarize the DC field by averaging over mJ states. We do not consider such averaging here.

For the above cases where unpolarized fields were considered, results are the same whether or not one considers hyperfine structure. For the case of polarized Stark shifts, as we consider here, results depend on the particular $|F, m_F\rangle$ level in question. Trapped ion experiments have demonstrated stray field compensation below 2.4 V/m [35], which we use for our calculations. DC Stark shifts in the $X_1 0^+$ manifold are much larger from adjacent rotational levels than from states in the $X_2 1$ manifold. The $|X_1 0^+, v=0, J=0, F=1/2, m_F=1/2\rangle$ has a shift of -3.7 mHz, and because of a near cancellation the $|X_1 0^+, v=8, J=1, F=1/2, m_F=1/2\rangle$ state has a shift of 0.12 mHz. The transition between $F=1/2$ states additionally has the advantage of having no electric quadrupole moment.

Spectroscopy states within the $X_1 0^+$ ground state are also relatively immune to large Zeeman shifts due to a lack of orbital or spin angular momentum. The remaining effects produce shifts on the order of a nuclear magneton. The effective Zeeman Hamiltonian can be written in as:

$$H_Z = g_I \mu_N \mathbf{B} \cdot \mathbf{I} + g_r \mu_B \mathbf{B} \cdot \mathbf{R} + g_s \mu_B \mathbf{B} \cdot \mathbf{S} \quad (4)$$

TABLE II: Other Shifts from Electric Fields^a

Effect	Ground	Excited	Diff.	σ/f_{0s}
Light Shift	$<10^{-5}$	$<10^{-5}$	$<10^{-5}$	$<10^{-4}$
DC Stark	-0.21	0.01	0.22	0.51
Quadrupole	0	0	0	0

^a Electric field shifts for a 2.4 V/m field. All values in mHz except the final column, the fractional uncertainty divided by 10^{-18} .

The three interactions originate from the proton nuclear spin, rotational and electron spin magnetic moments interacting with a magnetic field \mathbf{B} , where g_I , g_r , and g_s are the associated g factors. Here we assume magnetic field instabilities are linearly polarized along the z direction, \mathbf{B}_z . The matrix elements for each interaction are adapted from [23] and the total expected Zeeman shifts are presented in Table III, where we assume magnetic field control at the level of 3 nT uncertainty [36]. The first order proton nuclear spin interaction will have a differential shift of 21 mHz. The second order shift, calculated from the off-diagonal terms in F, depends on the strength of the nuclear-spin rotation interaction, signified by the coupling constant: c_I . A smaller c_I will lead to stronger mixing of F states. Because this constant was not calculated, we assume a conservative value of 10 kHz, based on the c_I value of 100 kHz measured in the much faster rotating OH molecule [37]. The second order Zeeman shift is almost two orders of magnitude smaller than the first order shift: 0.18 mHz.

The rotational magnetic moment arises from the charged nuclei rotating. The electrons adiabatically rotating with the nuclei create an equal magnitude magnetic moment in the opposite direction. However, rotational-electronic coupling leaves behind a residual magnetic moment [38, 39]. A $|J=0\rangle$ state does not possess a rotational magnetic moment, so we only concern ourselves with the $|X_1 0^+, v=8, J=1\rangle$ state. Given the similar reduced mass, equilibrium bond length and iso-electronic structure, we use the rotational g factor measured for the antimony hydride (SbH) molecule, $g_r \sim -0.001$ [40]. This yields a first order Zeeman shift of 34 mHz. Due to the large rotational splitting, off-diagonal elements in J can be ignored. Off-diagonal coupling in F will lead to a second order Zeeman shift of 0.15 mHz.

Neither $X_2 1$ nor $X_1 0^+$ possess an orbital magnetic moment, and the $X_1 0^+$ state will have no electron spin interaction to first order. However, second order rotational-electronic couplings will cause mixing, introducing a contribution from the Bohr magneton-sized magnetic moment in $X_2 1$. In certain cases, the degree of mixing can be very strong in higher vibrational states [41, 42]. The Ω -doubling in $X_2 1$ is primarily caused by rotational-electronic coupling to nearby electronic states of $\Omega = \pm 1$ and can therefore be used to predict the degree of mixing in $X_1 0^+$ using second order perturbation theory. In a Hund's case (c) basis, the Ω -doublet splitting for a given

TABLE III: Zeeman Shifts^a

Effect	\bar{f}	\bar{f}/f_{0s}	σ_f/f_{0s}
First Order			
Rotation	0	0	<0.2
Nuclear Spin	0	0	<0.2
Electron Spin	0	0	<0.2
Total	0	0	0.2
Second Order			
Rotation	0.15	0.35	0.35
Nuclear Spin	0.18	0.42	0.42
Total	0.33	0.77	0.55

^a Zeeman shifts for a 3 nT magnetic field. The first column represents the average frequency shift in mHz. The final columns are the fractional shift and uncertainty divided by 10^{-18} , respectively.

rotational state J is given by:

$$\Delta T_{ef} = qJ(J+1) \quad (5)$$

Assuming X_{21} is uniquely perturbed by X_{10^+} , the Ω -doubling interaction strength q can be approximated as [43]:

$$q = \frac{2B^2 \langle X_{21} | J_a | X_{10^+} \rangle}{\Delta E} \quad (6)$$

where $J_a = L + S$, ΔE is the spin-orbit splitting, B is the rotational constant in X_{21} and:

$$\langle X_{21} | J_a | X_{10^+} \rangle = J_a(J_a + 1)^{0.5} \quad (7)$$

We justify the use of this approximation by comparing a measured value of q for SbH to a computed value of q with the experimentally determined rotational constant and spin-orbit splitting inputted into Eq. 6 [44]. The expression is accurate to within one part in one thousand, demonstrating that molecules of this kind are well-described by Hund's case (c). Because the lowest angular momentum state in X_{21} is $J = 1$, $|X_{10^+}, v = 0, J = 0\rangle$ will not couple significantly to X_{21} . Taking the data from Ornellas et al. for TeH^+ , the B constant for $v = 8, J = 1$ is 4.68 cm^{-1} and a ΔE for $|X_{10^+}, v = 8\rangle - |X_{21}, v = 8\rangle$ of 914 cm^{-1} , yields an Ω -doubling constant of 0.096 cm^{-1} . Exclusive of any coupling to additional excited states, this results in a degree of mixing between $\Omega = 0$ and $\Omega = 1$ on the order of $\sqrt{2}B/\Delta E$, leading to a first order shift of 55 mHz. Similar to the previous interactions considered, the second order contribution will be suppressed due to the large spin-orbit splitting and large rotational constant. Therefore, we omit its contribution.

Although the first order Zeeman shifts are on the order of 10-100 mHz, these shifts can be effectively mitigated by averaging over transitions with opposite shifts,

yielding an average frequency shift of \bar{f} [45]. Specifically, we consider driving transitions between the stretched states $|X_{10^+}, v = 0, J = 0, F = 1/2, m_F = 1/2\rangle$ and $|X_{10^+}, v = 8, J = 1, F = 1/2, m_F = -1/2\rangle$ as well as $|X_{10^+}, v = 0, J = 0, F = 1/2, m_F = -1/2\rangle$ and $|X_{10^+}, v = 8, J = 1, F = 1/2, m_F = 1/2\rangle$. We note that $F = 1/2$ in $J = 1$ has a g factor with opposite sign. Using this technique, Nicholson et al. demonstrate a fractional uncertainty in the first order Zeeman shift of 2×10^{-19} . The first order Zeeman shifts can also be eliminated by instead working with $^{125}\text{TeH}^+$. The ^{125}Te has a nuclear spin of $1/2$, which will produce integer F states. Driving transitions between states of $m_F = 0$ will be insensitive to Zeeman shifts to first order. The combination of second order Zeeman shifts from Table III is 0.33 mHz. Summing the total electric and magnetic shift uncertainties in quadrature yields a total fractional uncertainty of 8×10^{-19} .

In addition to the favorable electronic properties mentioned above, TeH^+ has some additional attractive experimental features. The ^{130}Te isotope is readily available with 34% natural abundance. TeH^+ can be prepared via resonance enhanced multi-photon ionization of neutral TeH . Due to the low melting point of tellurium, a bright and stable source of TeH can be made using a Smalley-type source using molten tellurium [46, 47]. Also, neither ^{130}Te nor H possesses a nuclear quadrupole moment, leading to a simpler determination of molecular constants. Lastly, $^{130}\text{TeH}^+$ is a relatively heavy ion, which is favorable for reducing second order Doppler shifts to below the level of systematic uncertainty presented here [48]. In addition, the mass of $^{130}\text{TeH}^+$ is fairly close to that of Ba^+ , making this atomic ion an ideal candidate for sympathetic cooling and quantum logic state readout [49].

In conclusion, we have presented TeH^+ as a candidate for setting new limits on the variation of μ . TeH^+ presents several favorable factors that meet a strict criteria allowing for both simple and efficient state preparation and high sensitivity to μ . Although the smallest laboratory limit on the variation of μ was performed using an atom, this limit comes at the cost of implementing a model that relates a variation in μ with a variation in the nuclear magnetic moment [50]. In comparison, the variation of μ with vibrational frequency is more straightforward. The current molecular limit on the variation of μ is $5.6 \times 10^{-14}/\text{yr}$ [51]. Optical overtone spectroscopy on a single TeH^+ ion shows extraordinary potential to surpass these limits, with an expected reach beyond the level of 10^{-17} .

ACKNOWLEDGMENTS

This work was supported by AFOSR Grant No. FA9550-13-1-0116, NSF Grant No. PHY-1404455, and NSF GRFP DGE-1324585

-
- [1] J.-P. Uzan, *Living Reviews in Relativity* **14**, 2 (2011).
- [2] P. Jansen, H. L. Bethlem, and W. Ubachs, *The Journal of Chemical Physics* **140**, 010901 (2014).
- [3] V. V. Flambaum, D. B. Leinweber, A. W. Thomas, and R. D. Young, *Physical Review D* **69**, 115006 (2004).
- [4] J. Bagdonaite, M. Daprà, P. Jansen, H. L. Bethlem, W. Ubachs, S. Muller, C. Henkel, and K. M. Menten, *Physical Review Letters* **111**, 231101 (2013).
- [5] R. M. Godun, P. B. R. Nisbet-Jones, J. M. Jones, S. A. King, L. A. M. Johnson, H. S. Margolis, K. Szymaniec, S. N. Lea, K. Bongs, and P. Gill, *Physical Review Letters* **113**, 210801 (2014).
- [6] N. Huntemann, B. Lipphardt, C. Tamm, V. Gerginov, S. Weyers, and E. Peik, *Physical Review Letters* **113**, 210802 (2014).
- [7] D. Demille, S. Sainis, J. Sage, T. Bergeman, S. Kotochigova, and E. Tiesinga, *Physical Review Letters* **100**, 043202 (2008), arXiv:0709.0963v1.
- [8] D. Hanneke, R. A. Carollo, and D. A. Lane, *Physical Review A* **94**, 050101 (2016).
- [9] M. G. Kozlov, *Physical Review A - Atomic, Molecular, and Optical Physics* **80**, 022118 (2009), 0905.1714.
- [10] C. Chin and V. V. Flambaum, *Physical Review Letters* **96**, 230801 (2006).
- [11] V. V. Flambaum and M. G. Kozlov, *Physical Review Letters* **98**, 240801 (2007).
- [12] T. Zelevinsky, S. Kotochigova, and J. Ye, *Physical Review Letters* **100**, 043201 (2008).
- [13] M. Kajita, G. Gopakumar, M. Abe, and M. Hada, *Physical Review A - Atomic, Molecular, and Optical Physics* **85**, 062519 (2012).
- [14] J. C. J. Koelemeij, D. W. E. Noom, D. de Jong, M. A. Haddad, and W. Ubachs, *Applied Physics B* **107**, 1075 (2012).
- [15] N. B. Khanyile, G. Shu, and K. R. Brown, *Nature Communications* **6**, 7825 (2015).
- [16] A. K. Hansen, O. O. Versolato, L. Kłosowski, S. B. Kristensen, A. Gingell, M. Schwarz, A. Windberger, J. Ullrich, J. R. C. López-Urrutia, and M. Drewsen, *Nature* **508**, 76 (2014).
- [17] P. F. Staunum, K. Højbjerg, P. S. Skyt, A. K. Hansen, and M. Drewsen, *Nature Physics* **6** (2010).
- [18] C.-Y. Lien, C. M. Seck, Y.-W. Lin, J. H. Nguyen, D. A. Tabor, and B. C. Odom, *Nature Communications* **5**, 4783 (2014).
- [19] C.-w. Chou, C. Kurz, D. B. Hume, P. N. Plessow, D. R. Leibbrandt, and D. Leibfried, *Nature* **545**, 203 (2017).
- [20] T. Schneider, B. Roth, H. Duncker, I. Ernsting, and S. Schiller, *Nature Physics* **6**, 275 (2010).
- [21] F. Wolf, Y. Wan, J. C. Heip, F. Gebert, C. Shi, and P. O. Schmidt, *Nature* **530**, 457 (2016).
- [22] L. Gonçalves dos Santos, A. G. S. de Oliveira-Filho, and F. R. Ornellas, *The Journal of Chemical Physics* **142**, 024316 (2015).
- [23] J. Brown and A. Carrington, *Rotational Spectroscopy of Diatomic Molecules* (Cambridge University Press, 2003), ISBN 0-511-05787-3.
- [24] R. J. Le Roy, *Journal of Quantitative Spectroscopy and Radiative Transfer* **186**, 167 (2017).
- [25] A. B. Alekseyev, H.-P. Liebermann, R. M. Lingott, O. Bludský, and R. J. Buenker, *The Journal of Chemical Physics* **108**, 7695 (1998).
- [26] S. Yu, D. Fu, A. Shayesteh, I. E. Gordon, D. R. T. Appadoo, and P. Bernath, *Journal of Molecular Spectroscopy* **229**, 257 (2005).
- [27] O. Shestakov, R. Gielen, A. Pravilov, K. Setzer, and E. Fink, *Journal of Molecular Spectroscopy* **191**, 199 (1998).
- [28] L. Hollberg, C. W. Oates, E. Anne Curtis, E. N. Ivanov, S. A. Diddams, T. Udem, H. G. Robinson, J. C. Bergquist, R. J. Rafac, W. M. Itano, et al., *IEEE Journal of Quantum Electronics* **37**, 1502 (2001).
- [29] E. Riis and A. G. Sinclair, *Journal of Physics B: Atomic, Molecular and Optical Physics* **37**, 4719 (2004).
- [30] E. Peik, T. Schneider, and C. Tamm, *Journal of Physics B: Atomic, Molecular and Optical Physics* **39**, 145 (2006), 0511168.
- [31] P. Dubé, A. A. Madej, A. Shiner, and B. Jian, *Physical Review A* **92**, 042119 (2015).
- [32] P. R. Stollenwerk, M. G. Kokish, and B. C. Odom, *Manuscript in Preparation* (2017).
- [33] J. W. Farley and W. H. Wing, *Physical Review A* **23**, 2397 (1981).
- [34] R. Krems, B. Friedrich, and W. C. Stwalley, *Cold Molecules: Theory, Experiment, Applications* (CRC Press, 2009), ISBN 9781420059045.
- [35] N. Huntemann, C. Sanner, B. Lipphardt, C. Tamm, and E. Peik, *Physical Review Letters* **116**, 063001 (2016).
- [36] A. A. Madej, P. Dubé, Z. Zhou, J. E. Bernard, and M. Gertsvolf, *Physical Review Letters* **109**, 203002 (2012).
- [37] J. Brown, M. Kaise, C. Kerr, and D. Milton, *Molecular Physics* **36**, 553 (1978).
- [38] J. F. Ogilvie, J. Oddershede, and S. P. A. Sauer (2000), chap. The Rotational g Factor of Diatomic Molecules in State $^1\Sigma^+$ or 0^+ , pp. 475–536.
- [39] F. Raab, T. Bergeman, D. Lieberman, and H. Metcalf, *Physical Review A* **24**, 3120 (1981).
- [40] V. Stackmann, K. Lipus, and W. Urban, *Molecular Physics* **80**, 635 (1993).
- [41] M. Borkowski, P. Morzyński, R. Ciuryło, P. S. Julienne, M. Yan, B. J. DeSalvo, and T. C. Killian, *Physical Review A* **90**, 032713 (2014).
- [42] B. H. McGuyer, C. B. Osborn, M. McDonald, G. Reinaudi, W. Skomorowski, R. Moszynski, and T. Zelevinsky, *Physical Review Letters* **111**, 243003 (2013).
- [43] G. Bujin and C. Linton, *Journal of Molecular Spectroscopy* **147**, 120 (1991).
- [44] M. Beutel, K. Setzer, O. Shestakov, and E. Fink, *Journal of Molecular Spectroscopy* **179**, 79 (1996).
- [45] T. Nicholson, S. Campbell, R. Hutson, G. Marti, B. Bloom, R. McNally, W. Zhang, M. Barrett, M. Safronova, G. Strouse, et al., *Nature Communications* **6**, 6896 (2015).
- [46] C. M. Neal, G. A. Breaux, B. Cao, A. K. Starace, and M. F. Jarrold, *Review of Scientific Instruments* **78**, 075108 (2007).
- [47] M. G. Kokish, M. R. Dietrich, and B. C. Odom, *Journal of Physics B: Atomic, Molecular and Optical Physics* **49**, 035301 (2016).
- [48] J. Keller, T. Burgermeister, D. Kalincev, J. Kiethe, and T. E. Mehlstäubler, *Journal of Physics: Conference Series*

- ries **723**, 2 (2015).
- [49] J. B. Wübbena, S. Amairi, O. Mandel, and P. O. Schmidt, *Physical Review A* **85**, 043412 (2012).
- [50] V. V. Flambaum and A. F. Tedesco, *Physical Review C* **73**, 055501 (2006).
- [51] A. Shelkovernikov, R. J. Butcher, C. Chardonnet, and A. Amy-Klein, *Physical Review Letters* **100**, 150801 (2008).